

Scaling Properties of Pinned Interfaces in Fractal Media

Alexander S. Balankin,* Orlando Susarrey, and Jesús Márquez Gonzáles

Sección de Posgrado e Investigación, ESIME, Instituto Politécnico Nacional, México D.F., 07738

(Received 15 April 2002; published 3 March 2003)

Experimental data for rupture lines and wetting fronts in various kinds of paper suggest that the scaling properties of interfaces pinned in such fractally correlated media are governed by the fractal dimension, D , of the medium. Specifically, the phenomenological relation $\zeta = D - (d - 1)$, where d is the spatial dimension of the system, satisfactorily describes the local roughness exponent, ζ , of a pinned interface. The relation is supported by analysis of the competition between an elastic restoring force and correlated pinning force in an elastic fractal media, under the assumption that the pinning force correlations decaying with distance, r , as $r^{-\eta}$ with $0 < \eta = d - D < 1$.

DOI: 10.1103/PhysRevLett.90.096101

PACS numbers: 68.35.Fx, 05.40.-a, 05.70.Ln, 61.43.Hv

It is well established that for sufficiently strong driving, the interface feels an effective smeared out thermal noise and its fluctuations present all the typical phenomena of scale invariance of driven systems [1–3]. Specifically, a moving interface may be characterized by the fluctuations of the height around its mean value. So, a basic quantity to look at is the global interface width, $W(L, t) = \{ \langle [h(x, t) - \langle h \rangle_L]^2 \rangle_L \}^{1/2}$, where the $\langle \cdots \rangle_L$ denotes an average over all x in a system of size L and $\{ \cdots \}$ denotes an average over different realizations. It has been found, that in many cases, $W(L, t)$ scales according to the Family-Vicsek ansatz [1–3] as $W(L, t) = t^{\alpha/z} f(L/t^{1/z})$, where the scaling function $f(y)$ behaves as y^α , if $y \ll 1$, or $f(y) = \text{const}$, if $y \gg 1$. The global roughness exponent α and the dynamic exponent z characterize the universality class of the dynamic roughening model under study [1–3]. The Family-Vicsek ansatz can be also applied to describe the scaling behavior of the local interface width, $w(\Delta, t) = \{ \langle [h(x, t) - \langle h \rangle_\Delta]^2 \rangle_\Delta \}^{1/2} = t^{\zeta/z} f(\Delta/t^{1/z})$, where $\langle \cdots \rangle_\Delta$ denotes an average over x in a window of size Δ [1]. In the absence of any characteristic length in the system, the local behavior of interface is characterized by the same scaling exponents as the global one, but generally, the local roughness exponent ζ is less or equal to the global one, i.e., $\zeta \leq \alpha$ [2].

In the opposite case of weak driving, the quenched nature of spatial heterogeneities becomes apparent and the interface reaches a pinned state, characterized by completely different roughness exponents [1]. Experimental values of the local roughness exponent for a large variety of significantly different systems vary in the relatively narrow interval $0.4 \leq \zeta \leq 0.9$ [1–5]. This, together with the prediction of some popular theoretical models, has led to the universality hypothesis, according to which ζ can take only certain universal values [1,6,7]. At the same time, the universality hypothesis has been questioned in some theoretical [8,9] and experimental [10] works. The purpose of the present work is to understand the effect of long-range correlations in fractal media on the scaling properties of pinned interfaces.

To gain insight into this problem we have performed a study of interfaces formed in five papers characterized by different fractal dimensions of their fiber structure and their pore space (see Table I and Refs. [5,11–15]). It is important to note that three kinds of “filtro” paper and “secante” paper are made from the same wood fibers (see Table I), while the “toilet” paper is made from fibers of a different kind. It should also be noted that the thickness, areal density, density, and the porosity are not constant for a given paper; rather the values vary from sample to sample in accordance with a normal distribution with means given in Table I, where $\rho_r = \rho/\rho_o$ is the relative density, ρ_o is the fiber density, and $P = 100(1 - \rho_r)$ is the porosity. Furthermore, we note that according to criterion [14], the toilet paper should be treated as a two-dimensional fiber network ($d = 2$), while the filtro and secante papers should be treated as three-dimensional networks ($d = 3$).

The fractal dimension, D_{fiber} , of the fiber network for each paper was determined using β radiography (for details, see [5,11]) from the scaling behavior of the two-point density fluctuation correlation function [see Fig. 1(a)], as defined by

$$C(\vec{R}) = \langle [m(\vec{x}) - \bar{m}][m(\vec{x} + \vec{R}) - \bar{m}] \rangle \propto |\vec{R}|^{-\eta}, \quad (1)$$

where m is the local basis weight, \bar{m} its average, and the brackets denote an average over the sample. The scaling behavior (1) is observed within the interval $\ell_0 < R < \xi_c$, where ℓ_0 is the average fiber width and ξ_c is the correlation length, $135 \leq \xi_c/\ell_0 \leq 840$ (see Table I). The density correlation exponent $\eta = d - D_{\text{fiber}}$ displays considerable variations from sample to sample in accordance with a normal distribution: see Fig. 1(b). Furthermore, as follows from the plot in Fig. 1(c), the relative densities of the papers satisfy the fractal relation

$$\rho = \rho_o \left(\frac{\xi_c}{\ell_c} \right)^{-\eta} \quad (2)$$

with constant ratio $\xi_c/\ell_c = \exp(2.5) = 12.18$ for four

TABLE I. Properties of five kinds of paper and scaling exponents of rupture lines and wetting fronts.

	“Filtro” paper ($d = 3$ [5]) with			(4) “Secante”	(5) “Toilet”
	(1) Open Porosity	(2) Medium Porosity	(3) Closed Porosity	Paper ($d = 3$ [5])	Paper [5,18] ($d = 2$ [17])
Thickness, mm	0.321	0.251	0.211	0.338	0.110
Areal density, kg/m ²	0.1284	0.1034	0.1024	0.1999	0.0368
Density, kg/m ³	400.09	411.95	485.76	591.28	334.55
Young modulus, GPA	1.12 ± 0.15	1.57 ± 0.20	2.02 ± 0.25	3.55 ± 0.35	0.17 ± 0.07
Fiber width, ℓ_0 , mm	0.04 ± 0.03	0.04 ± 0.03	0.04 ± 0.03	0.04 ± 0.05	0.03
Fiber density, kg/m ³	1494	1494	1494	1494	...
ξ_c , mm [from Eq. (1)]	6 ± 2	14 ± 5	20 ± 7	22 ± 9	34 ± 10
η [expt. (1)]	0.53 ± 0.05	0.51 ± 0.05	0.45 ± 0.04	0.37 ± 0.03	0.25 ± 0.03
$\ell_c = \xi_c/12.15$, mm	0.49	1.15	1.65	1.81	?
$D_{\text{fiber}} = d - \eta$	2.47 ± 0.05	2.49 ± 0.05	2.55 ± 0.04	2.63 ± 0.03	1.75 ± 0.03
D_{fiber} [expt. (2)]	2.47	2.49	2.55	2.63	1.75 (box)
ζ_{crack} (3)	0.47	0.49	0.55	0.63	0.75
ζ_{crack} (expt.)	0.45 ± 0.01	0.48 ± 0.01	0.56 ± 0.01	0.65 ± 0.03 [5]	0.75 ± 0.05
α_{crack} (expt.)	0.62 ± 0.05	0.67 ± 0.05	0.80 ± 0.05	$\alpha = \zeta$ [5]	...
Relative density	0.2681	0.2761	0.3255	0.3956	?
Porosity, %	73.2	72.4	67.5	60.4	?
ζ_{wet} (expt.)	0.785 ± 0.035	0.76 ± 0.03 [13]	0.70 ± 0.03	0.63 ± 0.03 [13]	0.5 ± 0.1
D_{pore} (5)	2.79	2.76	2.70	2.63	1.5
D_{pore} (4)	2.78	2.77	2.72	2.65	?

kinds of the papers studied. (Here ℓ_c is the characteristic size of the fiber network; see Table I.)

Experiments were performed on rectangular paper sheets of different widths, $L = 5, 10, 15, 20$, and 25 cm, and of length 25 cm. Cracks were produced in a uniaxial tension test of specimens with a straight cut of length $0.25L$ [17], carried out on a 4505 INSTRON testing machine with a constant deformation rate (the crack roughness exponent does not depend on the deformation rate [13,17]). The wetting fronts were formed in imbibition experiments with black Chinese-ink solution (see [18]) carried out under carefully controlled temperature $T = 20 \pm 3^\circ\text{C}$ and humidity $38\% \pm 6\%$. Each experiment was repeated 30 times, so for each kind of paper we obtain 150 wetting fronts and 300 rupture lines (in sheets of five different widths). The rough interfaces were scanned in black and white in the bit map (*.bmp*) format [12]. Then, the profiles of each interface were plotted using Scion-Image software [12] as single-valued functions $h(x)$, see Figs. 2(a) and 2(b); in the case of overhangs $h(x)$ refers to the highest point at x . The scaling properties of each interface were studied using five different statistical methods adopted in the BENOIT 1.2 software [5,19]: the variogram $V = w^2(\Delta)$, roughness-length (root-mean-square roughness), power-spectrum, and wavelets methods, and the rescaled-range (R/S) analysis. The global roughness exponents were determined from the scaling behavior $W \propto L^\alpha$ [5].

Figures 2(c) and 2(d) show the fractal graphs obtained by the rescaled roughness (c) and variogram (d) methods

for rupture lines and wetting fronts, respectively. Notice that the spatial extent over which scaling is observed is of the order of magnitude of the scaling range of the correlations in the fiber network; see Table I. Statistical distributions of the local roughness exponents ζ_{crack} and ζ_{wet} are shown in Figs. 3(a) and 3(b), respectively. Furthermore, we find that wetting fronts in toilet paper and cracks in filtro papers display an anomalous roughness with $\alpha_{\text{crack}} > \zeta_{\text{crack}}$ [see Fig. 3(c) and Table I], while the wetting fronts in secante and filtro papers, as well as the cracks in secante paper, are statistically self-affine ($\alpha = \zeta$).

As follows from Fig. 3(d), there is a strong correlation between the crack local roughness exponent and the fractal dimension of fiber network, which can be fitted very nicely by the simple relation

$$\zeta_{\text{crack}} = 1 - \eta = D_{\text{fiber}} - (d - 1). \quad (3)$$

Figure 1(d) shows the graph of paper porosity versus the local roughness of the wetting front. Taking into account the Katz-Thomson relation for fractal porosity [20], namely,

$$P/100 = K D_{\text{pore}}^{-d}, \quad (4)$$

where $K = k(R_{\text{max}}/R_{\text{min}})$, k is a geometrical factor, and R_{min} and R_{max} are the minimum and maximum characteristic pore sizes. From the fitted equation in Fig. 1(d) it follows that $K = \exp(1.38) = 3.97$ while the relation between ζ_{wet} and the fractal dimension of the pore space can be presented in the form

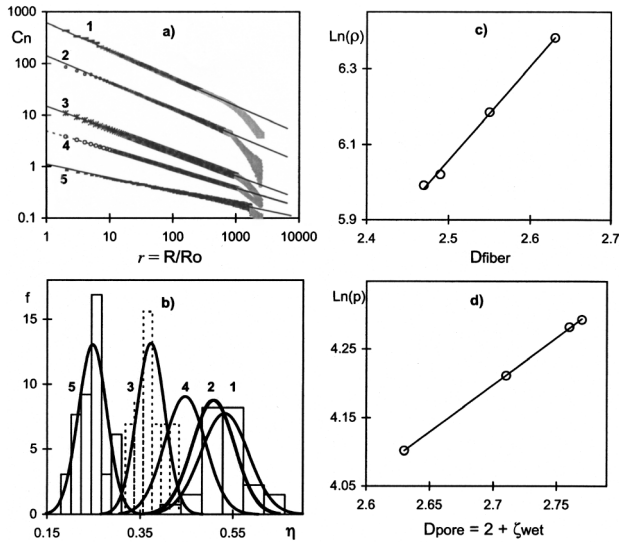


FIG. 1. (a) A log-log plot of the mass density correlation function $C_n = C(R)/C(R_0)$ versus $r = R/R_0$ ($R_0 = 1$ pixel = 0.02 mm, curves are shifted along axis C_n for clarity) and (b) statistical distributions of η for five papers numbered in Table I (bars: experimental data; solid lines: fitting by normal distribution with the help of @RISK 4.0 software [16]; the data bars for some papers are omitted for clarity). Graphs of (c) ρ versus D_{fiber} (circles: experimental data; solid line: fitting by equation $\ln(\rho) = 2.5D_{\text{fiber}} - 0.185$, with $R^2 = 0.9976$ and (d) P versus ζ_{wet} (dotted line: fitting by equation $\ln(P/100) = 1.38(\zeta_{\text{wet}} - 1)$, with $R^2 = 0.9827$).

$$D_{\text{pore}} = (d - 1) + \zeta_{\text{wet}}. \quad (5)$$

Now, one can easily check that the obvious relation $(\rho/\rho_0) + (P/100) = (12.18)^{D_{\text{fiber}}-d} + (3.97)^{D_{\text{pore}}-d} = 1$ is valid for all papers (see Table I).

It should be pointed out that the phenomenological relations (3) and (5) differ from the corresponding theoretical relationships obtained in Ref. [9]. To get a better insight into the nature of relations (3) and (5), we note that the saturated wetting fronts and cracks can be modeled as elastic objects pinned by quenched impurities [21]. So the roughness of a pinned interface is determined by competition between an elastic restoring force and a pinning force as

$$h(x, y) = \iint G(x - x_f, y - y_f) f(x_f, y_f) dx_f dy_f, \quad (6)$$

where f is the pinning force distribution, and G is the Green function for the equation of equilibrium of a pinned interface (see [22,23]). In fractal media the quenched pinning centers are expected to be correlated owing to the density-density correlations. Therefore, the pinning force two-point correlation function behaves as $\Gamma(r) \propto r^{-\eta}$, where $r = [(x - x_f)^2 + (y - y_f)^2]^{1/2}$ and $0 < \eta = d - D < 1$. This behavior is a characteristic of self-affine fractals [1]. Accordingly, we assume that the pinning force displays a self-affine scaling behavior

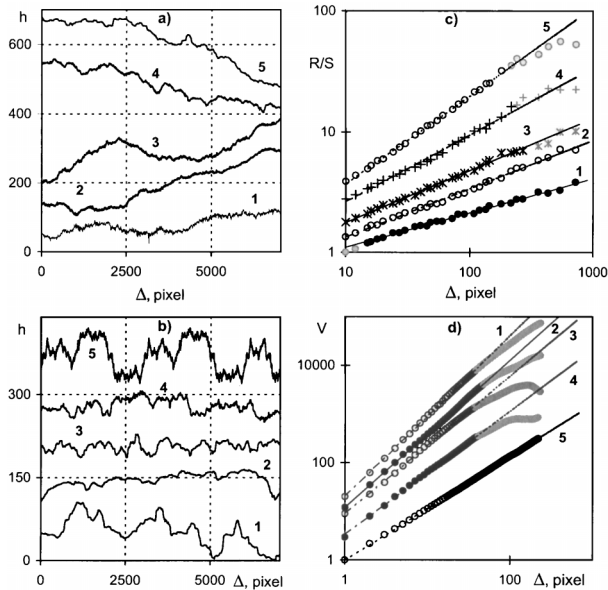


FIG. 2. Graphs of (a) rupture lines and (b) wetting fronts in five papers (1 pixel = 0.02 mm) and the corresponding fractal graphs, obtained by (c) the R/S (for rupture lines) and (d) variogram (for wetting fronts) methods (the plots are shifted along the abscissa for clarity). $R/S = \langle R(\Delta)/S(\Delta) \rangle$, where $R(\Delta)$ and $S(\Delta)$ are the range and the standard deviation of $h(x)$ within window Δ pixels, respectively; $V = w^2(\Delta)$.

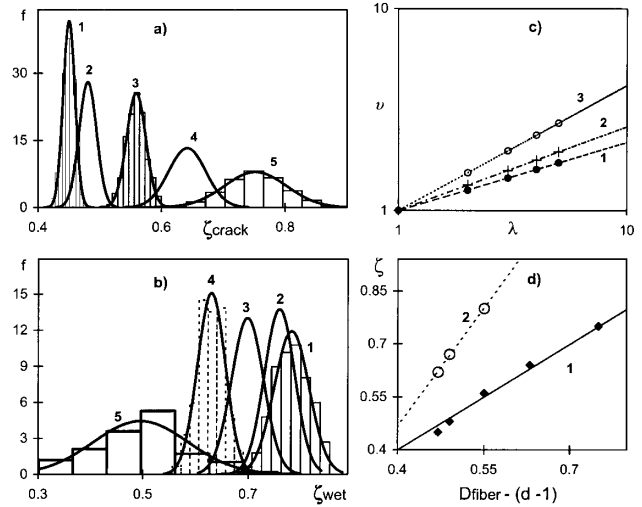


FIG. 3. Statistical distributions of (a) ζ_{crack} and (b) ζ_{wet} for five kinds of paper (see Table I); bars: experimental data; solid lines: fitting by normal distribution with the help of @RISK 4.0 software [16]. (c) Log-log plots of the normalized sample averaged global rupture line width $\nu = W(L)/W(L = 5 \text{ mm})$ versus the normalized paper sheet width $\lambda = L/(5 \text{ mm})$ for filter paper with (1) open, (2) medium, and (3) closed porosity; and (d) the graphs of (1) ζ_{crack} and (2) α versus $D_{\text{fiber}} - (d - 1)$ for five kinds of paper (solid line: fitting by equation $\zeta_{\text{crack}} = D_{\text{fiber}} - (d - 1)$; dotted line: fitting by equation $\alpha = 2.23\zeta_{\text{crack}} - 0.4262$).

$f(\lambda x, \lambda y) = \lambda^{-\eta} f(x, y)$. Such elastic interactions have been shown to significantly increase any long-range disorder correlations in the system [24]. A self-affine interface is asymptotically flat ($W/L \propto L^{\zeta-1} \rightarrow 0$ as $L \rightarrow \infty$). So, it is a good approximation to use the flat-surface Green function $G \propto r^{-1}$ [22]. To within the approximations we have made, Eq. (6) immediately gives the scaling relations $r \rightarrow \lambda r$, $G \rightarrow \lambda^{-1} G$, $f \rightarrow \lambda^{-\eta} f$, and $h \rightarrow \lambda^{1-\eta} h$. Thus, once again, we conclude that the local roughness exponent (ζ) of a pinned interface is related to the fractal dimension (D) of the media by $\zeta = 1 - \eta = D - (d - 1)$.

Accordingly, the fractal (box counting) dimension of a pinned self-affine interface ($D_{\text{int}} = d - \zeta$ [20]) is related to the fractal dimension (D) of correlated quenched noise by $D_{\text{int}} = (2d - 1) - D$. On the other hand, in the case of random media with short-range correlations, one may expect that the scaling properties of a moving interface are determined by a percolationlike mechanism (see [1]), which determines the universal value of ζ (see also [24]).

*Email address: abalankin@sni.conacyt.mx

- [1] A.-L. Barabási and H. E. Stanley, *Fractal Concepts in Surface Growth* (Cambridge University Press, Cambridge, 1995); J.-F. Gouyet, *Physics and Fractal Structures* (Springer, New York, 1996); P. Meakin, *Fractals, Scaling and Growth far from Equilibrium* (Cambridge University Press, New York, 1998).
- [2] J. J. Ramasco, J. M. López, and M. A. Rodríguez, *Phys. Rev. Lett.* **84**, 2199 (2000).
- [3] F. Family and T. Vicsek, *J. Phys. A* **18**, L75 (1985); J. Krug, *Adv. Phys.* **46**, 139 (1997).
- [4] B. B. Mandelbrot, D. E. Passoja, and A. J. Paullay, *Nature (London)* **308**, 721 (1984); J. M. López and J. Schmittbuhl, *Phys. Rev. E* **57**, 6405 (1998), and references therein.
- [5] A. S. Balankin and D. Morales M., in *Emergent Nature: Patterns, Growth and Scaling in the Sciences*, edited by M. M. Novak (World Scientific, London, 2001), pp. 345–356.
- [6] S. V. Buldyrev *et al.*, *Phys. Rev. A* **45**, R8313 (1992); L. A. N. Amaral *et al.*, *Phys. Rev. E* **51**, 4655 (1995).
- [7] E. Bouchaud, G. Lapasset, and J. Planés, *Europhys. Lett.* **13**, 73 (1990); A. Parisi, G. Caldarelli, and L. Pietronero, *Europhys. Lett.* **53**, 304 (2000), and references therein.
- [8] A. S. Balankin, *Eng. Fract. Mech.* **57**, 135 (1997), and references therein.
- [9] Different models of interface roughening in medium with correlated quenched noise lead to different relations between ζ and the noise correlation exponent: see, for example, E. Medina, T. Hwa, M. Kardar, and Y.-Ch. Zhang, *Phys. Rev. A* **39**, 3053 (1989); J. G. Amar, P.-M. Lam, and F. Family, *Phys. Rev. A* **43**, 4548 (1991); S. V. Buldyrev *et al.*, *Phys. Rev. A* **43**, 7113 (1991); Ch.-H. Lam, L. M. Sander, and D. E. Wolf, *Fractals* **1**, 1 (1993); M. Sahimi, *J. Phys. I (France)* **4**, 1263 (1994); X. Zhang, M. A. Knackstedt, D. Y. C. Chan, and L. Paterson, *Europhys. Lett.* **34**, 121 (1996); N.-N. Pang, *Int. J. Mod. Phys. B* **12**, 1921 (1998); R. Cafiero, cond-mat/9811072.
- [10] P. McNulty, L. V. Meisel, and P. J. Cote, *Phys. Rev. A* **46**, 3523 (1992); V. Y. Milman, R. Blumenfeld, N. A. Stelmashenko, and R. Ball, *Phys. Rev. Lett.* **71**, 204 (1993); F. Dossou and R. Gauvin, *Fractals* **2**, 249 (1994); A. S. Balankin, *Int. J. Fract.* **76**, R63 (1996); A. S. Balankin *et al.*, *ibid.* **87**, L37 (1997); A. S. Balankin, G. Urrionagoitia, and L. H. Hernandez, *Phys. Lett. A* **297**, 376 (2002).
- [11] N. Provatas, M. J. Alava, and T. Ala-Nissila, *Phys. Rev. E* **54**, R36 (1996); M. Myllys *et al.*, cond-mat/0105234.
- [12] <http://www.sciocorp.com> (Scion-Image, 1999).
- [13] A. S. Balankin *et al.*, *Proc. R. Soc. London, Ser. A* **455**, 2565 (1999).
- [14] K. J. Niskanen and M. J. Alava, *Phys. Rev. Lett.* **73**, 3475 (1994); E. K. O. Hellén, M. J. Alava, and K. J. Niskanen, *J. Appl. Phys.* **81**, 6425 (1997).
- [15] Papers have been widely used to study the kinetic roughening of interfaces in paper wetting, fracturing, and combustion experiments [5,7,9]. Most of the experiments with interface roughening in paper seem to produce a self-affine interface, but the numerical value of the exponents often bears little resemblance to the standard universality classes and/or associated models of interface pinning in random media. See, for example, J. Kertész, V. Horváth, and F. Weber, *Fractals* **1**, 67 (1993); V. K. Horváth and H. E. Stanley, *Phys. Rev. E* **52**, 5166 (1995); A. S. Balankin and O. Susarrey, *Int. J. Fract.* **81**, R27 (1996); A. S. Balankin *et al.*, *ibid.* **79**, R63 (1996); T.-H. Kwon, *Fractals* **5**, 121 (1997); A. S. Balankin *et al.*, *Int. J. Fract.* **90**, L57 (1998); A. S. Balankin, D. Morales M., and I. Campos, *Philos. Mag. Lett.* **80**, 503 (2000); A. S. Balankin and D. Morales M., *ibid.* **81**, 495 (2001).
- [16] <http://www.palisade.com> (@RISK 4.0, Palisade, 2002).
- [17] A. S. Balankin, O. Susarrey, and A. Bravo, *Phys. Rev. E* **64**, 066131 (2001).
- [18] A. S. Balankin, A. Bravo O., and D. Morales M., *Philos. Mag. Lett.* **80**, 1367 (2000).
- [19] <http://www.trusoft-international.com> (BENOIT 1.2, 1999); W. Seffens, *Science* **285**, 1228 (1999).
- [20] J. Feder, *Fractals* (Plenum Press, New York, 1988).
- [21] A. Tanguy, S. Krishnamurthy, P. Abry, and S. Roux, cond-mat/9908212.
- [22] L. D. Landau and E. M. Lifshitz, *Theory of Elasticity* (Pergamon Press, Oxford, 1958).
- [23] F. M. Borodich and A. Yu. Volovikov, *Proc. R. Soc. London, Ser. A* **456**, 1 (2000).
- [24] J. Schmittbuhl and J.-P. Vilotte, *Physica (Amsterdam)* **270A**, 42 (1999).